Available online at www.sciencedirect.com
ScienceDirect
International Journal of Pharmaceutics 340 (2007) 76–83
INTERNATIONAL JOURNAL OF PHARMACEUTICS
www.elsevier.com/locate/ijpharm

Combining SEM, TEM, and micro-Raman techniques to differentiate between the amorphous molecular level dispersions and nanodispersions of a poorly water-soluble drug within a polymer matrix

Evangelos Karavas [a,b], Manolis Georgarakis [b], Aristides Docoslis [c], Dimitrios Bikiaris [d,*]

[a] *Pharmathen S.A., Pharmaceutical Industry, Dervenakion Str. 6, Pallini Attikis, 153 51 Attiki, Greece*
[b] *Section of Pharmaceutics and Drug Control, Department of Pharmacy, Aristotle University of Thessaloniki, 541 24 Thessaloniki, Greece*
[c] *Department of Chemical Engineering, Queen's University at Kingston, Kingston, Ont., Canada K7L 3N6*
[d] *Laboratory of Organic Chemical Technology, Department of Chemistry, Aristotle University of Thessaloniki, 541 24 Thessaloniki, Greece*

Received 31 October 2006; received in revised form 5 March 2007; accepted 19 March 2007
Available online 30 March 2007

Abstract

The aim of the present study was to experimentally examine whether poorly water-soluble drugs dispersed in a polymeric matrix exist as amorphous nanodispersions or molecularly dispersed compounds. Felodipine (Felo) dispersed in PVP matrix (solid dispersion) was used as a model drug in this study. Drug/polymer ratios have an impact on the drug average particle size, morphology and dissolution profile while solid dispersions containing up to 50 wt% Felo are completely amorphous. SEM, TEM micrographs, and micro-Raman mapping reveal that Felo is dispersed in the form of nanoparticles into the PVP matrix. Due to the high spatial resolution of TEM, it was established that these nanoparticles are not uniform particles, but rather agglomerates of individual particles with sizes smaller than 5–10 nm. Moreover, micro-Raman mapping allowed us to observe the size and spatial distribution of domains where the drug existed as molecularly or nanodispersed. Experimental evidence presented in this work contradicts the common belief that amorphous poorly water-soluble drugs exist only in the state of molecular dispersion inside a polymer matrix by showing that both types of dispersions (molecular-level and nanodispersions) can coexist.

Keywords: Poor water-soluble drugs; Solid dispersions; Amorphous nanodispersions; SEM; TEM; Raman

1. Introduction

In pharmaceutical technology there exist numerous drug substances, including new chemical entities, that in spite of their high therapeutic effectiveness, are characterized by poor water solubility. The latter limits their potential uses in formulating bioavailable pharmaceutical products. In all those cases, the rate limiting factor for drug absorption becomes the dissolution rate of the active ingredient in the gastro-intestinal liquids (Hörter and Dressman, 2001). Therefore, the enhancement of oral bioavailability of such poor water-soluble drugs and the preparation of solid oral dosage forms is currently one of major objectives and greatest challenges in the area of new formulations development. 'Solid dispersion' is one of the earlier, yet still favorable, approaches for overcoming this limitation. Owing to its simplicity from the manufacturing and process scalability standpoints, solid dispersion has become one of the most active and promising research areas of great interest to pharmaceutical companies. Furthermore, such formulations possess considerable advantages over other commonly used techniques, especially micronization. Hence it is expected that the popularity of solid dispersions will grow rapidly (Serajuddin, 1999). The term solid dispersion refers to solid state mixtures, prepared through the dispersion, typically by solvent evaporation or melt mixing, of one or more active ingredients in an inert carrier matrix (Chiou and Riegelmann, 1971). In these dispersions, the drug can be present in a fully crystalline state (in the form of coarse drug particles), in a semicrystalline state, and in fully amorphous state (in the form of a fine particle dispersion, or molecularly distributed within the carrier). Such systems prove to be very effective for enhancing the dissolution rate of low solubility drugs.

* Corresponding author. Tel.: +30 2310 997812; fax: +30 2310 997667.
E-mail address: dbic@chem.auth.gr (D. Bikiaris).

0378-5173/$ – see front matter © 2007 Elsevier B.V. All rights reserved.
doi:10.1016/j.ijpharm.2007.03.037

Poly(ethylene glycol) (PEG) and polyvinylpyrrolidone (PVP) are the most used drug carriers for solid dispersion preparations (Tantishaiyakul et al., 1999; Van dem Mooter et al., 2001; Basit et al., 2001; Groves et al., 1984; Naima et al., 2001; Oaya et al., 2003) due to their strong hydrophilic properties and their capability to form molecular adducts with many compounds. The presence of hydroxyl or carbonyl groups in the repeat units of these polymers tend to increase the water-solubility (Trapani et al., 1999; Damian et al., 2002; Hideshi and Hisakazu, 1997) and stability (Damian et al., 2002; Gupta et al., 2005) of the drug and also improve its bioavailability (Kushida et al., 2002). It is accepted nowadays that the glassy state of a drug compound dispersed in such polymer matrices is the most desired state, since it improves its dissolution rate and hence drug absorption (Kaushal et al., 2004). Despite the large number of published studies on solid dispersions (600–700), the nature of the drug amorphous state has been less well investigated, hence it is still not clear how the drug is dispersed within the matrix in the majority of cases (Craig, 2002). In most of the published technical reports on amorphous dispersions, it was only surmised by the authors that the drug is molecularly dispersed in the matrix carrier, however, no clear evidence has been provided.

In the present study two microscopic techniques, scanning electron microscopy (SEM) and transmission electron microscopy (TEM) were used in a complementary fashion (in conjunction with XRD), in order to precisely and adequately differentiate between drug molecular dispersions and nanodispersions in amorphous solid dispersions of poorly water-soluble drugs. Felodipine was used here as a model compound to represent a poorly water-soluble drug dispersed in polyvinylpyrrolidone (PVP) matrix. Since SEM and TEM can provide only optical evidence of the drug dispersion, micro-Raman spectroscopy was also employed for the chemical analysis of dispersed Felo into the PVP matrix.

2. Experimental

2.1. Materials

Felodipine (Felo) with an assay of 99.9% and particle size range 20–100 μm was obtained from PCAS (Longjumeau, France). Felo has a melting point of 143–145 °C, solubility in water approximately equal to 0.5 mg/l, and it is freely soluble in ethanol. Polyvinylpyrrolidone (PVP), type Kollidon K30, was obtained from BASF (Ludwigshafen, Germany). The PVP used had molecular weight of 50,000–55,000, $T_g = 167$ °C (DSC), moisture content 1.95% (TGA) and bulk density of 0.410 g/cm^3. All other materials and reagents were of analytical grade of purity.

2.2. Preparation of solid dispersion systems

PVP/Felo solid dispersion systems of 90/10, 80/20, 70/30 and 50/50 (w/w) were prepared by dissolution of accurately weighed dry substances in appropriate quantities of absolute ethanol. The solutions were mixed, ultrasonicated for 20 min, and then the solvent was fully evaporated under vacuum in a rotary evaporator at 60 °C for 1 h.

2.3. In vitro release profile

Release of Felo from the solid dispersion systems was measured by a modified dissolution apparatus II (paddles) USP. The test was performed in 37 ± 1 °C with a rotation speed of 100 rpm using 500 ml of 0.1 M phosphate buffer pH 6.5 containing 2% polysorbate 20. The instrumentation used for the dissolution test was an HPLC apparatus type DISTEK 2100B equipped with an auto sampler.

2.4. Solubility in water at 37 °C

A dissolution apparatus II of USP (paddles) type DISTEK was used. Samples of each system equivalent to 50 mg FEL were placed in the vessels into hard gelatin capsules under the following conditions: 500 ml H_2O, 50 rpm, 37 °C, 36 h. The capsules were placed into specific metallic nets in order to remain in the bottom of the vessel so that the measurements are taken under constant hydrodynamic conditions. After 36 h 50 ml per sample was removed, filtered through 0.2 μm, and the water was evaporated under vacuum on a rotary evaporator, BUCH Rotavapor R200 equipped with a vacuum controller model V-800 and a heating bath model B-490. The residues were dissolved in 5 ml absolute ethanol and assayed with the HPLC method described in European pharmacopoeia. The analysis was performed on a type Shimadzu instrument model LC-20-10A, at 237 nm using a C_{18} column. The disintegration time of the hard gelatin capsules cannot affect the results of the experiment, as it was less than 5 min. The experiment was performed in triplicate, while the R.S.D. per sample was found to be less than 1.5%.

2.5. X-ray diffraction (XRD)

XRD analysis were performed on randomly oriented samples, scanned over the interval 5–55° 2θ, using a Philips PW1710 diffractometer, with Bragg-Brentano geometry (θ, 2θ) and Ni-filtered Cu Kα radiation.

2.6. Scanning electron microscopy (SEM)

The morphology of the prepared solid dispersions was determined by a scanning electron microscope (SEM), type JEOL (JMS-840) equipped with an energy-dispersive X-ray (EDX) Oxford ISIS 300 micro-analytical system. For this examination, fractured samples of solid dispersions prepared by immersion in liquid nitrogen were used.

2.7. Transmission electron microscopy (TEM)

Electron diffraction (ED) and transmission electron microscopy (TEM) investigations were performed on ultra thin film samples of solid dispersions prepared by ultra-microtome deposited on copper grids. TEM micrographs were obtained using a JEOL 120 CX microscope operating at 120 kV. To avoid

the destruction of PVP films after exposure to electron irradiation, an adequate sample preparation is required and thin films were carbon coated.

2.8. Micro-Raman spectroscopy

Raman studies on felodipine formulations were performed by using a Jobin-Yvon/Horiba micro-Raman Spectrometer (Model: Labram), equipped with a 632 nm He/Ne laser source (30 mW), 1800 1/nm grating and an Olympus BX41 microscope system. Spectra collection was performed at room temperature under the following conditions: 100× microscope objective, 50 μm pinhole size, 200 μm slit width, and 5 s exposure time. Each spectrum represents the average of two measurements. Sample profiling (2D mapping) was performed under the same conditions at a step increment of 0.1 μm in both *x*- and *y*-directions. The samples were first ground to powder with a mortar and pestle and then spread flat on a glass microscope slide.

3. Results and discussion

Oral drug delivery continues to be the method of choice for drug administration into the blood stream. Effective drug delivery, however, requires that the candidate therapeutic agent first be dissolved in the gastrointestinal lumen. The wt% release of Felo from pure drug samples and PVP/Felo systems is presented in Fig. 1, as measured after 15 min from the onset of the experiments. For comparison, the solubility of Felo in these systems is also presented. The two parameters are expressed as a function of PVP concentration in the system. An impressive enhancement of dissolution and solubility is achieved for low concentrations of the drug. This behaviour could be explained by many factors, such as the modification of the particle size, the solid state properties (amorphous or crystalline), and the existence of interactions between the two components in the systems (Karavas et al., 2006a, in press). For PVP/Felo solid dispersion containing 50 wt% Felo, the dissolution profile and solubility are almost identical to that of pure Felo.

Fig. 2 illustrates the X-ray diffraction patterns of PVP, Felo and the prepared solid dispersions. Felo is a crystalline compound with a very strong diffraction peak at 2θ of 23.38° while

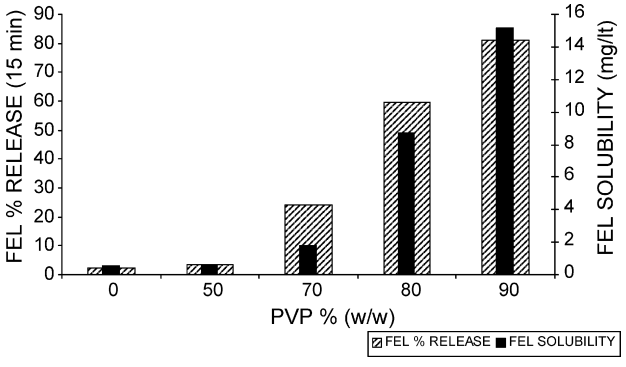

Fig. 1. Solubility and dissolution results of pure Felo and its solid dispersions as a function of PVP concentration obtained 15 min after the initiation of the experiments.

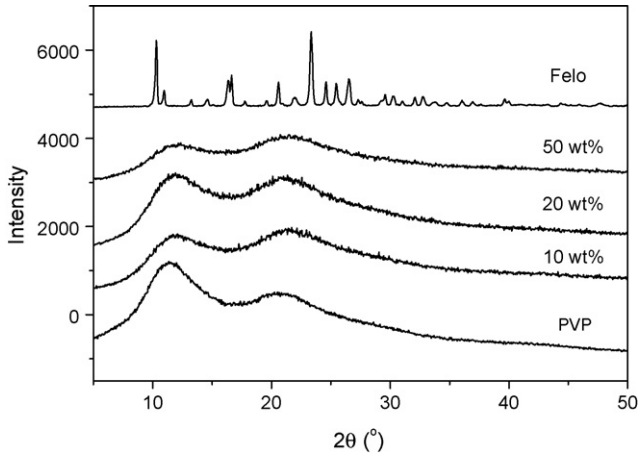

Fig. 2. XRD patterns of pure PVP, Felo, and its solid dispersions within PVP.

others presenting a lower intensity at 2θ of 10.32°, 11.0°, 16.32°, 16.64°, 20.6°, 22°, 24.6°, 25.5° and 26.6°. On the other hand, XRD patterns of PVP/Felo, showed the distinct broad peaks that observed in amorphous and high disorder materials that correspond to the diffraction pattern of pure PVP. Peaks that correspond to Felo were completely absent, confirming that the PVP matrix inhibited its crystallization.

Drugs in amorphous dispersions may be present in two forms: molecularly dispersed, a more desirable form that yields the highest dissolution rates, or nanodispersed with particle sizes preferably lower than 500 nm (Kanaze et al., 2006). These forms are difficult to be characterized or differentiated. Molecular dispersions can be detected by means of differential scanning calorimetry (DSC), where complete miscibility of the two components is characterized by a single glass transition temperature (T_g) that shifts between those of the pure drug and polymer as a function of the drug/polymer ratio in the mixture (Shmeis et al., 2004; Vasanthavada et al., 2005). However, in our studied PVP/Felo solid dispersions two well separated T_g's were recorded in the DSC thermograms (Karavas et al., 2005). The first one appeared at temperatures close to 30–50 °C and was assigned to the drug amorphous phase, while the second one, at temperatures between 160 and 170 °C, to the PVP phase. This is an indication that our prepared dispersions behave as inhomogeneous binary systems, i.e., Felo is not completely dispersed at a molecular level. Such systems, which are rather uncommon in bibliography, arouse the curiosity of how the drug is actually distributed into the polymer matrix.

In order to determine the morphology of PVP/Felo solid dispersions, SEM analysis of the samples was performed. SEM is a technique that can give information on the crystal shape and particle size of pure compounds, as well as their morphology in the solid dispersions (Bikiaris et al., 2005; Karavas et al., 2006b). Furthermore, it provides knowledge on the surface topography, without however being capable of revealing the underlying 3D structure, or helping us gain insight of the dynamics of the sample. Since Felo is the minor component in the PVP matrix, Felo particles well dispersed into PVP matrix are expected. As illustrated in Fig. 3, SEM micrographs reveal small irregularities that dominate on the surface of the samples.

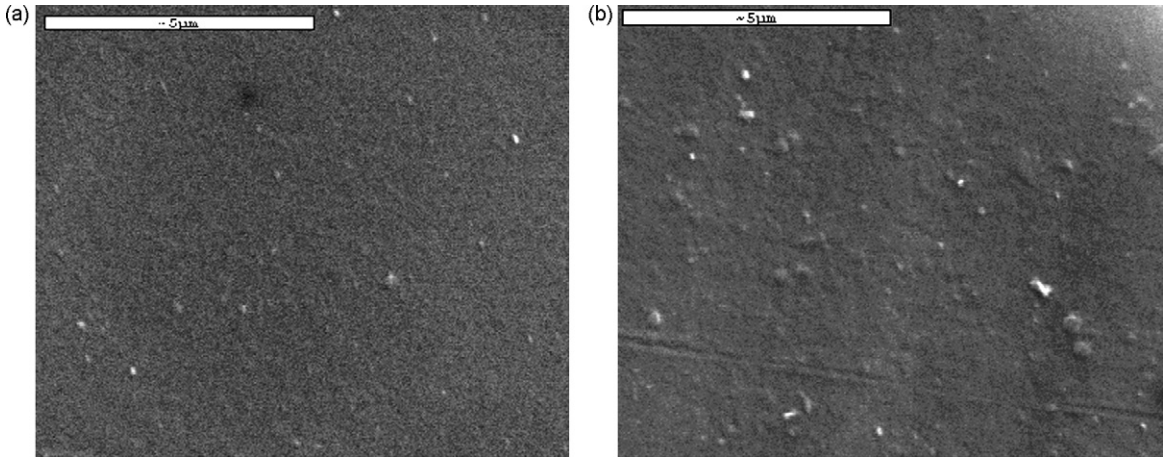

Fig. 3. Scanning electron micrographs of PVP/Felo solid dispersions: (a) 80/20 (w/w) and (b) 50/50 (w/w).

In spite of the surface anomalies, nano-sized (spherical) particles protruding from the polymer matrix are still distinguishable. These nanoparticles can be better distinguished by using secondary electrons (Fig. 4). Due to the existence of chloride in the Felo molecule, nanoparticles are recorded with lighter hue than that of the matrix. This is one more advantage of the SEM technique for the study of solid dispersions, since many drug molecules have chlorides or other detectable heavy molecules.

High-resolution scanning electron micrographs, acquired by using backscattering or secondary electrons, indicate the presence of particles with dimensions as small as 25–50 nm. The collected SEM micrographs suggest that the size of these nanoparticles depends on the felodipine wt% into the mixture. In the case of PVP/Felo 90/10 (w/w), the particle size of Felo ranges from 30 to 100 nm. These particles, however, are not easily discernible because of their fine dispersion in the PVP matrix and only by using the backscattering electrons we have some evidences of their existence (Fig. 4a). In solid dispersions corresponding to 80/20 (w/w) (PVP/Felo) mixing ratio, the particle size distribution appears to range between 50 and 130 nm, while in 50/50 (w/w) solid dispersions, distinct nanoparticles having diameters between 500 nm and larger than 1 μm (1–2 μm) can be readily observed (Fig. 4b). The prepared systems are closer to those described by Savolainen et al. (2002) who assumed that Felo exists as partial solid solution.

Analysis of the SEM micrographs obtained from PVP/Felo solid dispersions proves that Felo exists in the form of nanoparticles and does not attain molecular-level dispersion inside the PVP matrix. Despite the narrow distribution of Felo particle sizes, as measured from SEM micrographs obtained at various drug concentrations, it is not unlikely that a certain fraction of the dispersed Felo exists in the form of nanoparticles too small to be distinguished. Therefore, the main question does not cease to exist, i.e., whether some of the drug amount exists in molecular dispersion. Can these images exclude the presence of molecular dispersion? In such amorphous solid dispersions, the differentiation between molecular dispersion and nanodispersion is difficult. For this purpose, TEM might be the most useful technique to characterize the particle size distribution of Felo into PVP matrix. TEM has higher spatial resolution than SEM and is used extensively and successfully in the study of polymer blends and biological samples. However, it has never been used to study solid dispersions.

TEM photomicrographs obtained from PVP/Felo nanodispersions are presented in Fig. 5. The contrast of the sample can be enhanced by treatment with a heavy metal salt (negative

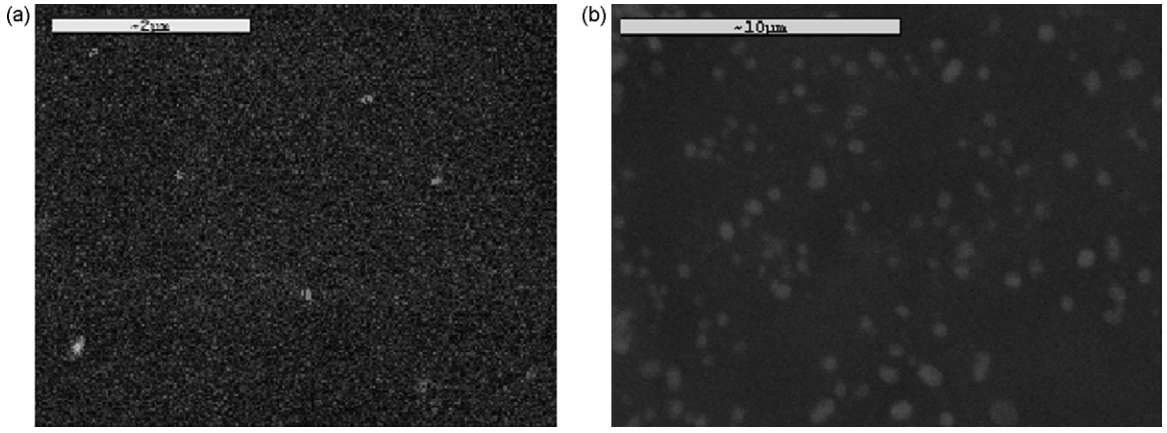

Fig. 4. Scanning electron micrographs of PVP/Felo solid dispersions taken with backscattering electrons: (a) 90/10 (w/w) and (b) 50/50 (w/w).

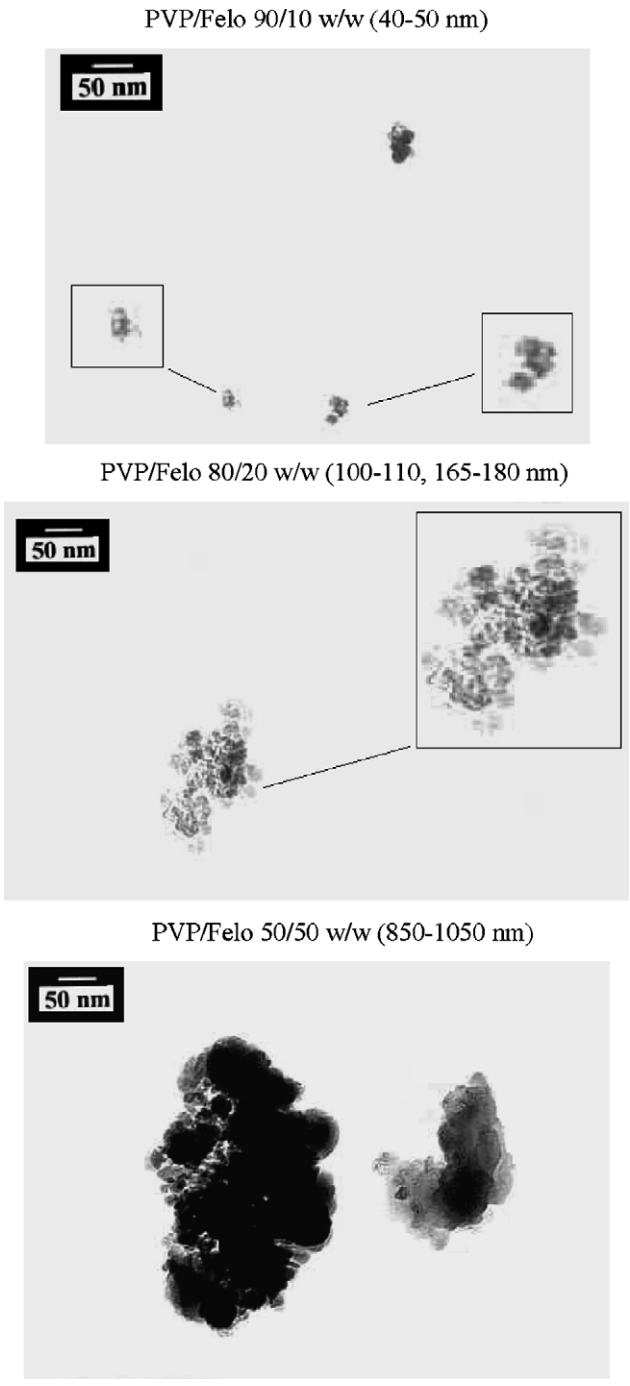

Fig. 5. Transmission electron photomicrographs of PVP/Felo nanodispersions at various drug concentrations.

stain). However, in the case of Felo this was not necessary by virtue of the chloride atoms contained in the molecules, which contribute to the generation of satisfactorily resolved images. Felo nanoparticles, appearing as black spots in the image, can be readily distinguished against the PVP matrix. The size distribution of these particles were directly affected by the drug ratio into the PVP matrix, as was already shown by SEM. In the solid dispersion of 90/10 (w/w) (PVP/Felo), particles were difficult detectable because of their fine dispersion and small size (20–130 nm). By increasing the Felo ratio in solid dispersions, particle sizes became progressively larger: they ranged between 50 and 200 nm, and 500–1000 nm in solid dispersions containing 20 and 50 wt% Felo, respectively. In all cases it was noticed that these nanoparticles are not uniform particles, as appeared in SEM micrographs, but rather aggregates of individual particles ranging in sizes from 5 to 10 nm. It should be recalled that particles with high specific surface area tend to aggregate; this trend becomes higher by increasing the drug concentration in the solid dispersion. The small size of the primary individual nanoparticles is possibly the main contributing factor to the high dissolution rate of Felo in nanodispersions with concentrations up to 20 wt% and mainly in 10 wt%. According to the Noyes–Whitney equation one of the most important factors to enhance the dissolution rate (DR) of a drug is to increase its available surface for dissolution and this can be achieved by several ways (Hörter and Dressman, 2001; Takeuchi et al., 2005; Wang et al., 2006). Thus, since the PVP/Felo solid dispersion containing 10 wt% Felo has the highest dissolution rate, it can be concluded that nanoparticle sizes lower than 150 nm are optimal towards achieving the highest dissolution rates for a poorly water-soluble drug.

The small individual nanoparticles observed with TEM constitute another basic morphological difference that could not be possibly distinguished with SEM. Furthermore, at high magnifications it can be seen that Felo nanoparticles have circular shape and consist of a dark core with a light shell. This may be either because of the shell being thinner than the core, or because of the formation of a concentration gradient at the boundaries (interfaces) between the two components. This becomes more obvious in the micrographs of PVP/Felo 90/10 and 80/20 (w/w) solid dispersions. TEM analysis, therefore, shows that a significant amount of Felo exists as nanodispersed into PVP. Higher magnification data from PVP thin film samples was not possible because of the instability of the specimens against the electron beam. Furthermore, irradiation raises the temperature locally, which causes drift of the specimen. These limitations can be mentioned as the main disadvantages of TEM technique to study the drug solid dispersions. Examining more carefully some of TEM micrographs it can be seen that the small nanoparticles, which normally prefer to aggregate in order to lower their surface energy, are sterically inhibited against crystal growth (as shown from XRD patterns) by a layer of protective PVP macromolecules. This is confirmed by photomicrographs taken at lower resolutions, as seen in Fig. 6, and can explain why in the particular solid dispersions Felo is dispersed in amorphous state.

From the above complementary study with SEM and TEM techniques it was proved that Felo forms nanoparticles inside the PVP matrix, each one of which constitutes an aggregate of smaller nanoparticles. However, it does not answered successfully the question of whether or not some drug content also exists in the form of molecular-level dispersion. An indication for this possibility was given in our previous DSC study which showed that a small part of the drug must disperse into the PVP phase, since the T_g's of the two components were shifted to different positions compared with those of the pure compounds (Karavas et al., 2005). For this reason the distribution of Felo

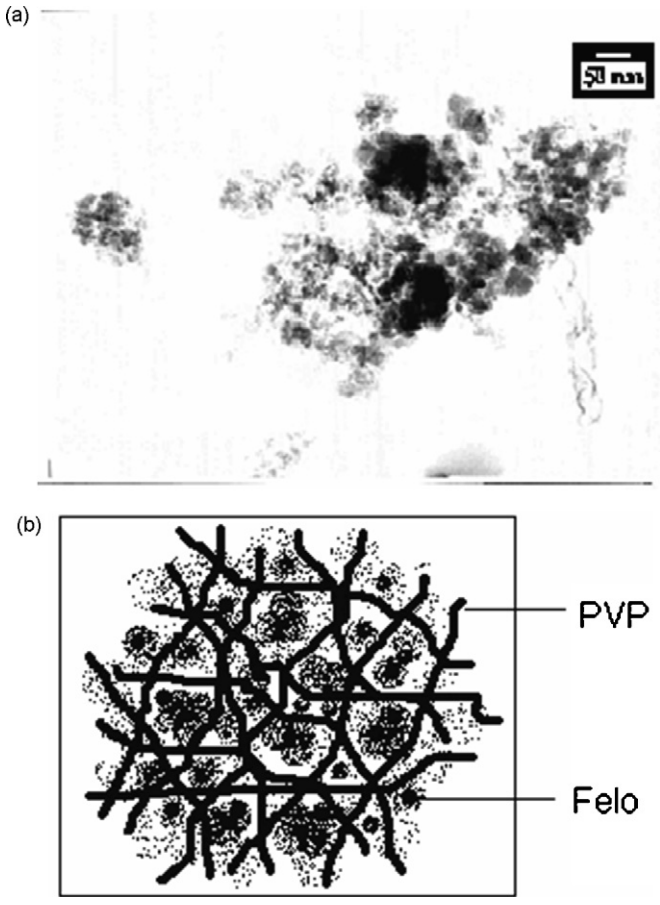

Fig. 6. (a) TEM photomicrograph of PVP/Felo nanodispersion from a sample containing 50 wt% Felo. (b) Schematic representation of the component distribution inside the observed aggregate.

into the PVP matrix was also studied by means of 2D micro-Raman spectroscopic mapping, which proved to be a helpful technique in the chemical characterization of the drug solid dispersions and mainly the drug polymorphism in such systems (Papageorgiou et al., 2006). The Raman spectra of pure Felo and PVP are shown in Fig. 7. Both spectra were obtained under the same experimental conditions and gave the same peak intensity (approximately 5500 a.u.) for the C–H stretching vibration mode (2929–2938 cm^{-1}). The Felo spectrum, however, shows a very strong characteristic peak at 1643 cm^{-1} (arrow in Fig. 7a), which is attributed to the free carbonyl group stretching mode. PVP also shows a similar band assignment, although significantly less intense (1100 a.u versus 46,600 a.u. for Felo) and slightly shifted to higher frequencies (1660 cm^{-1}). A characteristic peak for PVP, ascribed to the ring breathing mode, appears at 934 cm^{-1} (Lin-Vien et al., 1991). The latter, indicated by an arrow in Fig. 7b, is totally absent from the Felo spectrum.

XY (2D) micro-Raman spectroscopic mapping was performed at random locations on samples having Felo concentration of 10, 30 and 50 wt%. To avoid the effect of surface roughness that causes point-to-point variations in the spectrum intensity, the mapping results can be normalized if presented in terms of peak intensity ratios. Here, the ratio I_{1643}:I_{934} was selected as being the intensity ratio of two characteristic peaks,

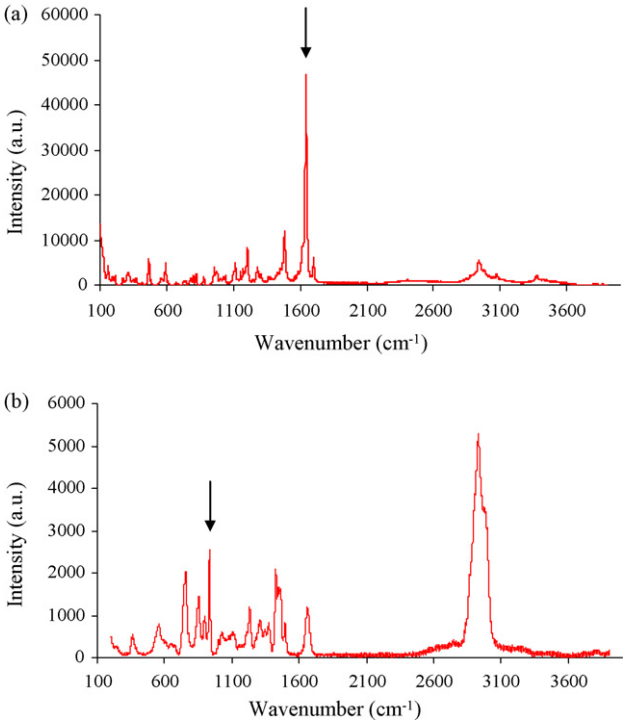

Fig. 7. Raman spectra of pure (a) felodipine and (b) PVP. The arrows indicate characteristic peaks used in the XY mapping of the samples.

each of which existing in only one of the components of the mixture. This parameter was found to be suitable for probing the spatial distribution of Felo in the samples. Figs. 8 and 9 present the results of XY mapping on samples at various Felo concentrations, expressed in terms of the I_{1643}:I_{934} ratio. From these mapping plots, one can immediately realize the strong effect of Felo:PVP mixing ratio on the resulting drug distribution in the sample. At concentration of 10 wt% Felo (Fig. 8), the mixing of the two components appears to be relatively uniform (light green areas), indicating that Felo exists in fine dispersion. This data suggest that a certain amount of Felo is dispersed in molecular level inside the PVP matrix, which is in agreement with a

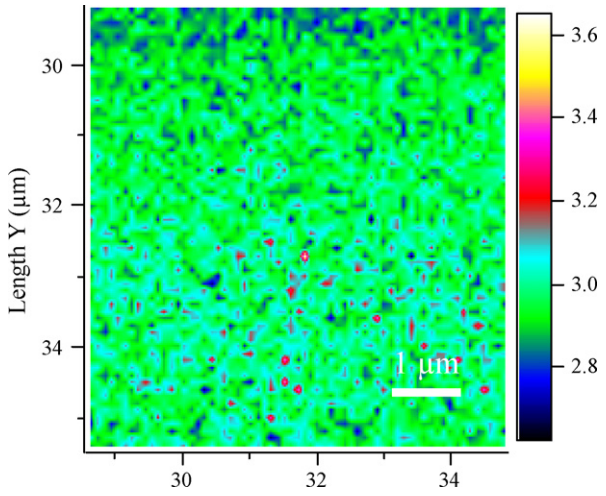

Fig. 8. XY micro-Raman mapping of Felo/PVP solid dispersion containing 10 wt% Felo. The scale bars indicate the intensity ratio I_{1643}:I_{934}.

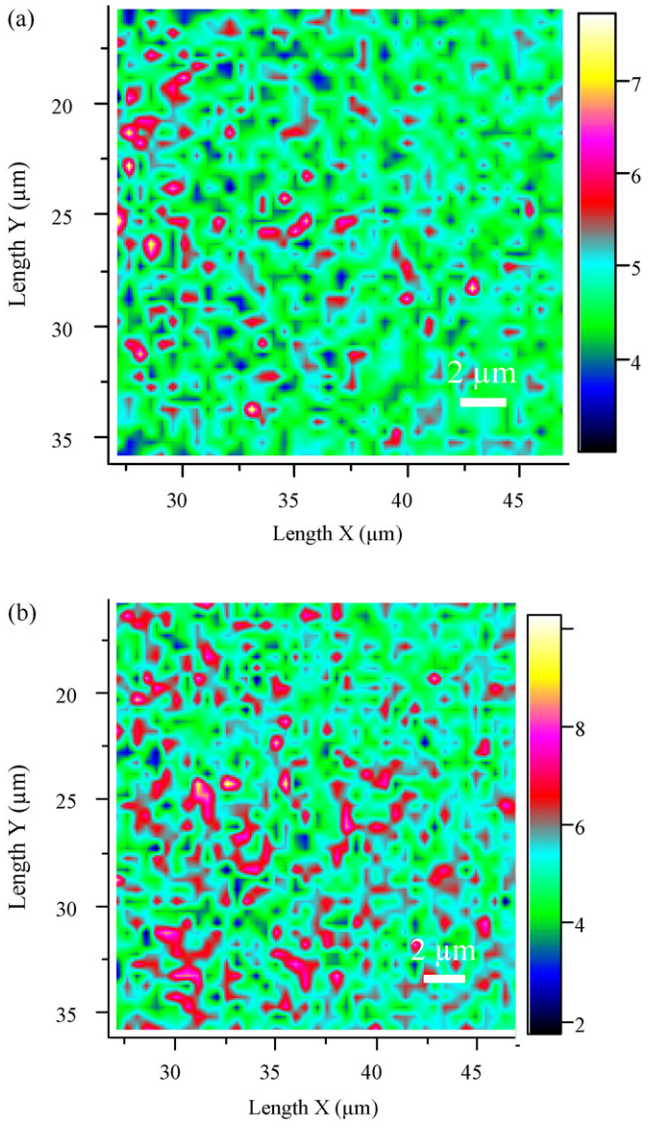

Fig. 9. XY micro-Raman mapping of Felo/PVP solid dispersions at various Felo concentrations: (a) 30 wt% and (b) 50 wt%. The scale bars indicate the intensity ratio I_{1643}:I_{934}.

recent study (Konno and Taylor, 2006). Spots of elevated Felo concentration, corresponding to a higher I_{1643}:I_{934} ratio, can also be observed. These spots, which appear to have dimensions in the order of 50–100 nm, is believed to represent Felo particles that have not achieved molecular-level dispersion in the polymer. The presence of Felo nanoparticles with dimensions smaller than, approximately, 50 nm should not be discounted; however, this level of resolution could not be attained by micro-Raman. Finally, pockets with submicron-level dimensions (dark blue areas), where less-than-average Felo concentration exists, are also visible. These observations agree with previous results obtained by SEM and TEM measurements, suggesting that a portion of the drug exists in the form of nanoparticles dispersed in the polymer matrix.

The size of the spots that correspond to elevated Felo concentration shows a marked increase in samples of 30 wt%. Felo (Fig. 9a), ranging approximately between 0.5 and 1.5 μm. At this concentration, the particles are still seen to exist as individual particles. When the average concentration of Felo in the mixture increases to 50 wt% (Fig. 9b), the particle size increases correspondingly. Moreover, it can be seen that the particle distribution can no longer be considered uniform, as a large number of these particles begin to fuse and form large domains, where Felo exists at higher-than-average concentrations. Additionally, as can be seen from the light green areas, where PVP and Felo coexist, the molecular dispersion of Felo decreases by increasing its content into solid dispersions.

4. Conclusions

A combination of experimental techniques, namely powder-XRD technique, scanning and transmission electron microscopies (SEM and TEM), and micro-Raman mapping reveal that Felo forms amorphous nanodispersions into a PVP polymer matrix over a drug concentration of 50 wt%. The particle sizes of the dispersed drug are strongly affected by the drug concentration and were found to lie in the range of 20–130 nm and up to about 1500–2000 nm for Felo concentrations of 10 and 50 wt%, respectively. According to the dissolution kinetics data, best performance was obtained by the dispersion system containing 10 wt% Felo, suggesting that optimal drug dissolution rates can be achieved when dispersions containing amorphous drug particles with sizes lower than 150 nm are used. TEM, having higher spatial resolution than SEM, reveals that these nanoparticles are aggregates of individually dispersed particles with sizes 5–10 nm. Micro-Raman spectroscopic mapping of the samples also confirms the existence of Felo-rich nano-domains, which increase in size with increasing drug concentration in the dispersions. However, it was also found that a portion of the drug exists in molecular level dispersion inside the PVP matrix. The present study demonstrates that TEM and micro-Raman are valuable techniques that can be used successfully for differentiating between the states of molecular dispersion and nanodispersion in amorphous solid dispersions of polymers. When combined with data on drug dissolution kinetics, particle size measurements obtained with TEM and micro-Raman spectroscopy can enhance our understanding of the effect of nanoparticle dispersion on drug release rates.

References

Basit, A.W., Newton, J.M., Short, M.D., Waddington, W.A., Ell, P.J., Lacey, L.F., 2001. The effects of polyethylene glycol 400 on gastrointestinal transit: implications for the formulation of poorly-water soluble drugs. Pharm. Res. 18, 1146–1150.

Bikiaris, D., Papageorgiou, G.Z., Stergiou, A., Pavlidou, E., Karavas, E., Kanaze, F., Georgarakis, M., 2005. Physicochemical studies on solid dispersions of poorly-water soluble drugs. Evaluation of capabilities and limitations of thermal analysis. Thermochim. Acta 439, 58–67.

Chiou, W.L., Riegelmann, S., 1971. Pharmaceutical applications of solid dispersion systems. J. Pharm. Sci. 60, 1281–1302.

Craig, D.Q.M., 2002. The mechanisms of drug release from solid dispersions in water-soluble polymers. Int. J. Pharm. 231, 131–144.

Damian, F., Blaton, N., Kinget, R., Van den Mooter, G., 2002. Physical stability of solid dispersions of the antiviral agent UC-781 with PEG 6000, Gelucire®44/14 and PVP K30. Int. J. Pharm. 244, 87–98.

Groves, M.J., Bassett, B., Sheth, V., 1984. The solubility of 17 β-oestradiol in aqueous polyethylene glycol 400. J. Pharm. Pharmacol. 36, 799–802.

Gupta, P., Thilagavathi, R., Chakraborti, A.S., Bansal, A.K., 2005. Role of molecular interaction in stability f Celecoxib-PVP amorphous systems. Mol. Pharm. 2, 84–391.

Hideshi, S., Hisakazu, S., 1997. Comparison of nicotinamide, ethylurea and polyethylene glycol as carriers for nifedipine solid dispersion systems. Chem. Pharm. Bull. 45, 1688–1693.

Hörter, D., Dressman, J.B., 2001. Influence of physicochemical properties on dissolution of drugs in the gastrointestinal tract. Adv. Drug Del. Rev. 46, 75–87.

Kanaze, F.I., Kokkalou, E., Niopas, I., Georgarakis, M., Stergiou, A., Bikiaris, D., 2006. Novel drug delivery systems for flavonoid compounds with enhanced solubility based on solid dispersions with polyvinypyrolidone and polyethyleneglycol. J. Appl. Polym. Sci. 102, 460–471.

Karavas, E., Ktistis, G., Xenakis, A., Georgarakis, E., 2005. Miscibility behavior and formation mechanism of stabilized felodipine-polyvinylpyrrolidone amorphous solid dispersions. Drug Dev. Ind. Pharm. 31, 473–489.

Karavas, E., Ktistis, G., Xenakis, A., Georgarakis, E., 2006a. Effect of hydrogen bonding interactions on the release mechanism of felodipine from nanodispensions with polyvinylpyrrolidone. Eur. J. Pharm. Biopharm. 63, 103–114.

Karavas, E., Georgarakis, E., Bikiaris, D., 2006b. Felodipine nanodispersions as active core for predictable pulsatile chronotherapeutics using PVP/HPMC blends as coating layer. Int. J. Pharm. 313, 189–197.

Karavas, E., Georgarakis, E., Sigalas, M.P., Avgoustakis, K., Bikiaris, D., in press. In situ investigation of the release mechanism of a sparingly water-soluble drug from its solid dispersions in hydrophilic carriers based on physical state of drug, particle size distribution and drug-polymer interactions. Eur. J. Pharm. Biopharm.

Kaushal, A.M., Gupta, P., Bansal, A.K., 2004. Amorphous drug delivery systems: molecular aspects, design, and performance. Crit. Rev. Therap. Drug Car. Syst. 21, 133–193.

Konno, H., Taylor, L.S., 2006. Influence of different polymers on the crystallization tendency of molecular dispersed amorphous felodipine. J. Pharm. Sci. 95, 2692–2705.

Kushida, I., Ichikawa, M., Asakawa, N., 2002. Improvement of dissolution and oral absorption of ER-34122, a poorly water-soluble dual 5-lipoxygenase/cyclooxygenase inhibitor with anti-inflammatory activity by preparing solid dispersion. J. Pharm. Sci. 91, 258–266.

Lin-Vien, D., Colthup, N.B., Fateley, W.G., Grasslli, J.G., 1991. The Handbook of Infrared and Raman Characteristic Frequencies of Organic Molecules, 1st ed. Academic Press, San Diego, CA.

Naima, Z., Siro, T., Juan-Manuel, G.D., Chantal, C., René, C., Jerome, D., 2001. Interactions between carbamazepine and polyethylene glycol (PEG) 6000: characterisations of the physical, solid dispersed and eutectic mixtures. Eur. J. Pharm. Sci. 12, 395–404.

Oaya, T., Lee, J., Park, K., 2003. Effects of ethylene glycol-based graft, star-shaped, and dendritic polymers on solubilization and controlled release of paclitaxel. J. Control. Release 93, 121–127.

Papageorgiou, G.Z., Bikiaris, D., Karavas, E., Politis, S., Docoslis, A., Park, Y., Stergiou, A., Georgarakis, E., 2006. Effect of physical state and particle size distribution on dissolution enhancement of Nimodipine/PEG solid dispersions prepared by melt mixing and solvent evaporation. APPS J. 8, E623–E631.

Savolainen, M., Khoo, C., Glad, H., Dahlqvist, C., Juppo, A.M., 2002. Evaluation of controlled-release polar lipid microparticles. Int. J. Pharm. 244, 151–161.

Serajuddin, A.T.M., 1999. Solid dispersion of poorly water-soluble drugs: early promises, subsequent problems and recent breakthroughs. J. Pharm. Sci. 88, 1058–1066.

Shmeis, R.A., Wang, Z., Krill, S.L., 2004. A mechanistic investigation of an amorphous pharmaceutical and its solid dispersions. Part I. A comparative analysis by thermally stimulated depolarization current and differential scanning calorimetry. Pharm. Res. 21, 2025–2030.

Takeuchi, H., Nagira, S., Tanimura, S., Yamamoto, H., Kawashima, Y., 2005. Solid dispersion containing amorphous indomethacin with fine porous silica particles by spray-drying method. Chem. Pharm. Bull. 53, 487–491.

Tantishaiyakul, V., Kaewnopparat, N., Ingkatawornwong, S., 1999. Properties of solid dispersions of piroxicam in polyvinylpyrrolidone. Int. J. Pharm. 181, 143–151.

Trapani, G., Franco, M., Latrofa, A., Pantaleo, M.R., Provenzano, M.R., Sanna, E., Maciocco, E., Liso, G., 1999. Physicochemical characterization and in vivo properties of zolpidem in solid dispersions with polyethylene glycol 4000 and 6000. Int. J. Pharm. 184, 121–130.

Van dem Mooter, G., Wuyts, M., Blaton, N., Busson, R., Grobet, P., Augustijns, P., Kinget, R., 2001. Physical stabilisation of amorphous ketoconazole in solid dispersions with polyvinylpyrrolidone K25. Eur. J. Pharm. Sci. 12, 261–269.

Vasanthavada, M., Tong, W.Q., Kislalioglu, M.S., 2005. Phase behaviour of amorphous molecular dispersions. II. Role of hydrogen bonding in solid solubility and phase separation kinetics. Pharm. Res. 22, 440–448.

Wang, L., Cui, F.D., Sunada, H., 2006. Preparation and evaluation of solid dispersions of nitrendipine prepared with fine silica particles using the melt mixing method. Chem. Pharm. Bull. 54, 37–43.